EUROPEAN ORGANIZATION FOR NUCLEAR RESEARCH (CERN)

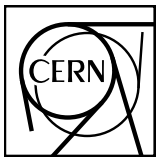

CERN-EP-2023-042
18 March 2023

Precision measurement of *CP* violation in the penguin-mediated decay $B_s^0 \to \phi\phi$

LHCb collaboration[†]

Abstract

A flavor-tagged time-dependent angular analysis of the decay $B_s^0 \to \phi\phi$ is performed using pp collision data collected by the LHCb experiment at the center-of-mass energy of 13 TeV, corresponding to an integrated luminosity of $6\,\text{fb}^{-1}$. The *CP*-violating phase and direct *CP*-violation parameter are measured to be $\phi_s^{s\bar{s}s} = -0.042 \pm 0.075 \pm 0.009\,\text{rad}$ and $|\lambda| = 1.004 \pm 0.030 \pm 0.009$, respectively, assuming the same values for all polarization states of the $\phi\phi$ system. In these results, the first uncertainties are statistical and the second systematic. These parameters are also determined separately for each polarization state, showing no evidence for polarization dependence. The results are combined with previous LHCb measurements using pp collisions at center-of-mass energies of 7 and 8 TeV, yielding $\phi_s^{s\bar{s}s} = -0.074 \pm 0.069\,\text{rad}$ and $|\lambda| = 1.009 \pm 0.030$. This is the most precise study of time-dependent *CP* violation in a penguin-dominated B meson decay. The results are consistent with *CP* symmetry and with the Standard Model predictions.

Submitted to Phys. Rev. Lett.

[†]Authors are listed at the end of this paper.

Probing the nature of *CP* violation is central to understanding how the matter-dominated universe came to existence. Precision studies of time-dependent *CP* asymmetries in $b \to c\bar{c}s$ decays at the e^+e^- B factories [1, 2] helped establish the CKM mechanism [3, 4] as the dominant source of *CP* violation in the Standard Model (SM). However, the amount of *CP* violation provided by this mechanism is insufficient to explain the observed matter-antimatter asymmetry [5]. Flavor-changing neutral current (FCNC) decays of B mesons are highly sensitive to new physics contributions entering via loop (penguin) processes and provide excellent opportunities to reveal new sources of *CP* violation.

The penguin-dominated decay $B_s^0 \to \phi\phi$, which proceeds via a $b \to s\bar{s}s$ transition, is a benchmark channel to study *CP* violation in FCNC decays at the LHCb experiment[1]. Time-dependent *CP* violation in this decay, arising from the interference between the direct decay and the decay after B_s^0 mixing, is characterized by the *CP*-violating phase $\phi_s^{s\bar{s}s}$ and the parameter $|\lambda|$, which is related to direct *CP* violation. In the SM, the phase $\phi_s^{s\bar{s}s}$ is expected to be very close to zero due to a cancellation of the mixing and decay weak phases [6–10], and the parameter $|\lambda|$ is expected to be close to unity, indicating vanishing direct *CP* asymmetry [7–11]. However, new physics contributions in the penguin decay or the B_s^0 mixing could significantly alter the values of $\phi_s^{s\bar{s}s}$ and $|\lambda|$ [12–15].

In addition, the $\phi\phi$ system in this decay is produced in three linear polarization states, and the effects of new physics may be polarization dependent [14, 15]. This is in contrast to the $B_s^0 \to J/\psi\phi$ decay, where potential new physics mainly affects the mixing process, since the decay amplitude is dominated by a tree-level $b \to c\bar{c}s$ diagram.

The LHCb collaboration has previously studied *CP* violation in the decay $B_s^0 \to \phi\phi$ [16–18]. The most precise measurements, $\phi_s^{s\bar{s}s} = -0.073 \pm 0.115\,(\text{stat}) \pm 0.027\,(\text{syst})\,\text{rad}$ and $|\lambda| = 0.99 \pm 0.05\,(\text{stat}) \pm 0.01\,(\text{syst})$ [18], are based on a data sample collected before 2017, corresponding to an integrated luminosity of $5\,\text{fb}^{-1}$. Due to the limited size of the data sample, a full polarization-dependent analysis was not performed. Instead, the *CP*-violating phases for the parallel and perpendicular polarization states were measured separately, with the phase of the longitudinal polarization fixed to zero. No evidence for polarization-dependent *CP* violation was observed.

This Letter reports an updated measurement of the *CP*-violation parameters in $B_s^0 \to \phi\phi$ decays using the full data sample of pp collisions collected with the LHCb detector at a center-of-mass energy of 13 TeV in 2015–2018 (Run 2), corresponding to an integrated luminosity of $6\,\text{fb}^{-1}$. The results are then combined with the LHCb result based on the data collected at 7 and 8 TeV in 2011 and 2012 (Run 1) [17], corresponding to an integrated luminosity of $3\,\text{fb}^{-1}$. Apart from the increased data sample size, this analysis also benefits from recent software improvements including new reconstruction algorithms for the vertex detectors that lead to a better decay-time resolution, and optimized flavor-tagging algorithms that increase the effective tagging efficiency. The flavor-tagged time-dependent angular analysis reported here largely follows the procedure described in Refs. [18]. New features related to the calibration of flavor tagging and decay-time resolution, and the modelling of decay-time acceptance are described in detail below. The increased sample size enables the *CP*-violation parameters in the decay $B_s^0 \to \phi\phi$ to be measured independently for all polarization states for the first time.

The LHCb detector is a single-arm forward spectrometer covering the pseudorapidity

[1]Charge-conjugation processes are implied throughout this Letter.

range $2 < \eta < 5$ and is described in detail in Refs. [19, 20]. The simulated events used in this analysis are produced with the software described in Refs. [21–27]. The online event selection is performed by a trigger [28], which consists of a hardware trigger followed by a two-stage software trigger. For this analysis, the hardware trigger selects hadron or muon candidates with high transverse momentum ($p_{\rm T}$). In the software trigger, $B^0_s \to \phi\phi$ candidates are selected either by identifying events containing a pair of oppositely charged kaons with an invariant mass close to that of the ϕ meson, or by using a three-body topological b-hadron trigger [29].

In the offline selection, $B^0_s \to \phi\phi$ candidates, with the ϕ mesons decaying to a K^+K^- pair, are reconstructed by combining four high-quality charged tracks compatible with originating from the same vertex and identified as kaons. All tracks are required to have a $p_{\rm T}$ above 0.4 GeV/c. Two K^+K^- pairs, each with an invariant mass within 20 MeV/c^2 of the known mass of the ϕ meson [30], are combined to form $B^0_s \to \phi\phi$ candidates and the product of their $p_{\rm T}$ is required to be above 1.2 GeV$^2/c^2$. The decay time of the B^0_s candidates must be larger than 0.3 ps. The $K^+K^-K^+K^-$ invariant mass, $m(K^+K^-K^+K^-)$, must fall in the interval [5000, 5800] MeV/c^2. Potential contamination from $B^0 \to \phi K^{*0}$ decays is largely suppressed by removing candidates that have a K^+K^- invariant mass within 30 MeV/c^2 of the known $K^*(892)^0$ mass [30] when the pion mass is assigned to a kaon candidate.

A multilayer perceptron (MLP) classifier [31,32] is used to further suppress background and improve the signal significance. The vertex fit χ^2 per degree of freedom, $p_{\rm T}$ and η of the B^0_s candidate, the cosine of the angle between the B^0_s momentum and its flight direction, as well as the $p_{\rm T}$ and η of the kaon and ϕ candidates are used as discriminating variables. The MLP classifier is trained using a sample of simulated $B^0_s \to \phi\phi$ decays representing the signal and a background data sample consisting of $B^0_s \to \phi\phi$ candidates with an invariant mass outside a $\pm 120\,{\rm MeV}/c^2$ window around the known B^0_s mass [30]. The k-fold method [33] with $k = 8$ is employed in the training of the MLP classifier. The lower threshold on the MLP output is chosen by maximizing the figure-of-merit defined as $N_s/\sqrt{N_s + N_b}$, where N_s is the expected signal yield in the signal region [5322, 5412] MeV/c^2 and N_b is the expected background yield in this region estimated by interpolating the number of candidates observed in the sideband regions [5100, 5160] MeV/c^2 and [5487, 5547] MeV/c^2. Roughly 3% of the events contain more than one candidate. In these cases one candidate is chosen at random, and the influence of this choice is found to be negligible.

Selected $B^0_s \to \phi\phi$ candidates in the mass range [5150, 5600] MeV/c^2 are used in subsequent analysis. The mass distribution of these candidates is shown in Fig. 1(a). Two sources of background are identified: the combinatorial background and a peaking background component from $\Lambda^0_b \to \phi K^- p$ decays due to misidentification of a proton as a kaon. A maximum-likelihood fit is performed to the mass distribution of selected $B^0_s \to \phi\phi$ candidates. The signal shape is described by the sum of a double-sided Crystal Ball function [34] and a Student's t-function [35] with all parameters fixed to the values estimated in the simulation except the peak position and resolution. The $\Lambda^0_b \to \phi K^- p$ background is described by a double-sided Crystal Ball function with the shape parameters fixed to the values determined using the RapidSim package [36]. The combinatorial background is represented by an exponential function. The yields of the three components, the position and resolution of the signal component and the slope of the background exponential function are allowed to vary in the fit. The $B^0_s \to \phi\phi$ signal yield is measured

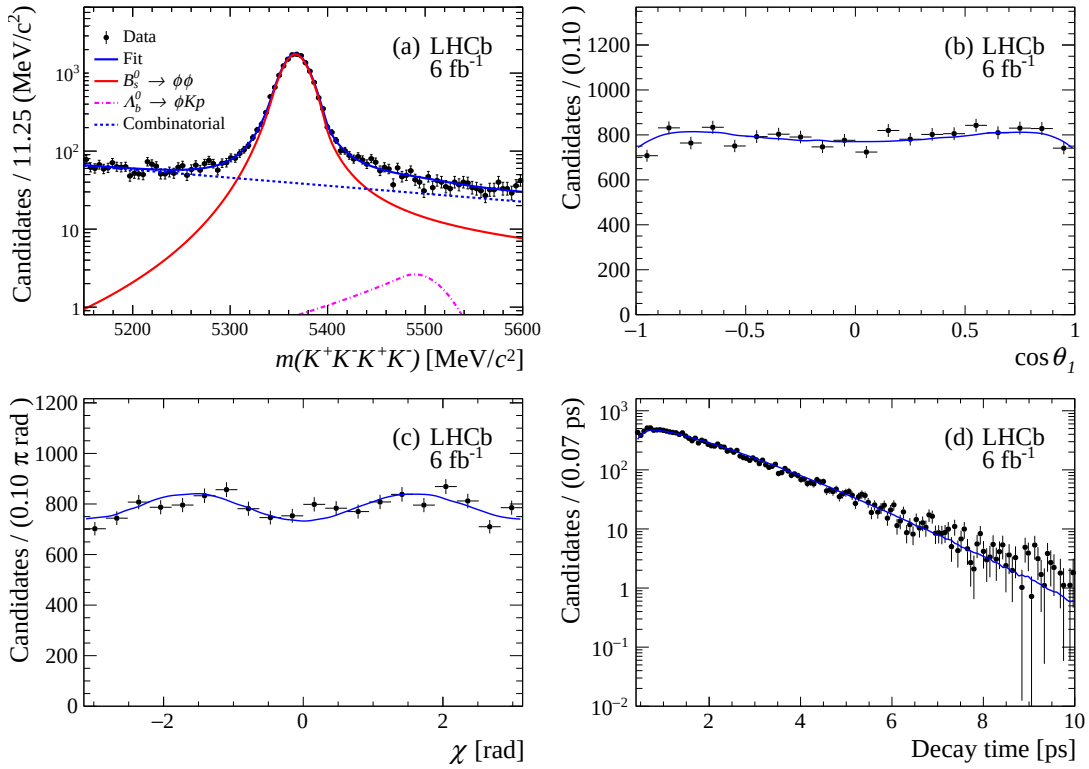

Figure 1: (a) Mass distribution of the $B_s^0 \to \phi\phi$ candidates, superimposed by the fit projections. (b-d) Background-subtracted distributions of angular variables ($\cos\theta_1$ and χ) and decay time, superimposed by the fit projections.

to be 15840 ± 140. Based on the result of the fit to the mass distribution, a signal weight is assigned to each candidate using the *sPlot* method [37]. These signal weights are subsequently used in a maximum-likelihood fit [38] to the decay-time and angular distributions in order to statistically subtract the background contribution.

The decay of a B_s^0 meson to the $K^+K^-K^+K^-$ final state can proceed via the $\phi\phi$, ϕf_0 and $f_0 f_0$ intermediate states. Due to the small phase space of the decay $f_0 \to K^+K^-$ and the narrow K^+K^- mass window used to select the ϕ candidates, the latter two contributions are highly suppressed and found to be negligible from an angular fit that accounts for these contributions. Thus in the subsequent analysis, only the $B_s^0 \to \phi\phi$ decay is considered. The differential decay rate is written as the sum of six terms, corresponding to contributions from the three polarization states and their interferences,

$$\frac{\mathrm{d}^4\Gamma(t,\vec{\Omega})}{\mathrm{d}t\mathrm{d}\vec{\Omega}} \propto \sum_{k=1}^{6} h_k(t) f_k(\vec{\Omega}) \,, \tag{1}$$

where t is the decay time of the B_s^0 meson, and $\vec{\Omega} = (\theta_1, \theta_2, \chi)$ denotes the helicity angles of the two K^+ mesons in the corresponding ϕ rest frame (θ_1, θ_2) and the angle between the two $\phi \to K^+K^-$ decay planes (χ). The angular functions $f_k(\vec{\Omega})$ are defined in Ref. [18]. The time-dependent functions $h_k(t)$ are given by

$$h_k(t) = N_k e^{-\Gamma_s t}\left[a_k \cosh\left(\frac{\Delta\Gamma_s}{2}t\right) + b_k \sinh\left(\frac{\Delta\Gamma_s}{2}t\right) + Qc_k \cos(\Delta m_s\, t) + Qd_k \sin(\Delta m_s\, t)\right] .$$

Here Q equals $+1$ (-1) for an initial B_s^0 ($\overline{B}_s^0$) state, Δm_s is the mass difference between the heavy and light B_s^0 mass eigenstates, $\Delta\Gamma_s$ is the decay width difference between the light and heavy mass eigenstates, and Γ_s is the average decay width. Ignoring *CP* violation in the B_s^0 mixing, in line with experimental measurements [39], the coefficients N_k, a_k, b_k, c_k and d_k are defined [18] in terms of the magnitudes $|A_i|$, phases δ_i, *CP*-violating phases $\phi_{s,i}$ and direct *CP*-violation parameters $|\lambda_i|$ for the three polarization states of the B_s^0 decay at $t = 0$, with $i = 0,\ \|,\ \perp$. The three amplitudes satisfy $|A_0|^2 + \left|A_\|\right|^2 + |A_\perp|^2 = 1$. The parameters $\phi_{s,i}$ and $|\lambda_i|$ are defined by the equation

$$\frac{q}{p}\frac{\bar{A}_i}{A_i} = \eta_i\,|\lambda_i|\,e^{-i\phi_{s,i}}\ , \tag{2}$$

where η_i is the *CP* eigenvalue of the polarization state i, q and p are complex numbers relating the B_s^0 mass eigenstates to the flavor eigenstates. A subset of parameters, chosen here as $(\phi_{s,i},\ |\lambda_i|,\ |A_0|^2,\ |A_\perp|^2,\ \delta_\perp - \delta_0,\ \delta_\| - \delta_0)$, can be determined by performing a maximum-likelihood fit to the distributions of t, $\vec{\Omega}$ and Q. In the SM-like case or new physics scenarios where *CP* violation is polarization independent, the set of *CP*-violation observables can be reduced to $\phi_{s,i} = \phi_s^{s\bar{s}s}$ and $|\lambda_i| = |\lambda|$. In this analysis, the above formalism is used to obtain both polarization-independent and polarization-dependent results, taking into account the experimental effects discussed below.

The detector acceptance and selection requirements lead to a nonuniform efficiency as a function of the angular variables, referred to below as the angular acceptance. This effect is accounted for through the use of normalization factors calculated with simulated signal events subject to the same selection criteria as the data. Weights are assigned to the simulated events to improve the agreement with the data, in the shape of the kaon $p_{\rm T}$ distribution. These weights are determined with an iterative algorithm [18, 40].

The reconstruction, trigger and selection requirements result in a decay-time dependent efficiency. A cubic spline function [41], with 7 knots at [0.3, 0.5, 1.0, 1.5, 2.0, 3.0, 8.0] ps and 9 coefficients, is employed to describe the decay-time dependent efficiency function, referred to below as the decay-time acceptance. One coefficient is fixed to unity for normalization, and all the other coefficients are free parameters in the fit to the data. Compared with the previous analysis in Ref. [18], which used $B_s^0 \to D_s^-\pi^+$ and $B^0 \to J/\psi K^{*0}$ decays as control channels to determine the decay-time acceptance, this method with free acceptance parameters simplifies the analysis without loss of precision for the physics parameters.

The dilution effect of the decay-time resolution on the B_s^0 oscillation is modelled by a Gaussian with a per-candidate width σ_t, which is related to the per-candidate decay-time uncertainty, δ_t, through a linear calibration function $\sigma_t = q_0 + q_1 \times \delta_t$. The parameters q_0 and q_1 are obtained using fictitious candidates formed of four prompt tracks from pp interactions, which have a decay time centered around 0. These prompt candidates are weighted to match the momentum and $p_{\rm T}$ distributions of the signal candidates and split into ten δ_t intervals. For each interval, the effective time resolution $\sigma_{t,i}$ is estimated by fitting the sum of three Gaussian functions with a common mean to the decay-time distribution of the prompt candidates and converting the resultant triple Gaussian into a single Gaussian that has the same damping effect on the observed B_s^0 oscillation amplitude [42]. A linear fit to the data points $(\delta_{t,i},\ \sigma_{t,i})$ for all intervals provides the estimates of q_0 and q_1. The reliability of this calibration method is verified using simulated samples of signal decays and prompt candidates. The effective decay-time resolution is found to be between 42 and 44 fs , depending on the data-taking year.

The initial flavor of a B_s^0 meson is inferred using both opposite-side (OS) [43] and same-side (SS) [44] tagging algorithms. Each of the two methods yields a tagging decision Q with a mistag probability κ for each B_s^0 candidate, where $Q = +1,\ -1$ or 0, if the candidate is classified as B_s^0, $\overline{B}_s^0$ or untagged, respectively. The mistag probability is calibrated using a linear function $\omega = p_0 + p_1 \times \kappa$ for the OS tagging and a quadratic function $\omega = p_0 + p_1 \times \kappa + p_2 \times \kappa^2$ for the SS tagging, where ω is the corrected mistag probability. The calibration of the OS mistag probability uses $B^+ \to J/\psi K^+$ decays, for which the value of ω in an interval of κ can be obtained from the numbers of correct and wrong decisions. The calibration of the SS mistag probability uses flavor-specific $B_s^0 \to D_s^- \pi^+$ decays, for which the value of ω in an interval of κ is estimated by fitting the decay-time distribution. Detailed descriptions of the calibration procedures can be found in Refs. [18, 40]. The effective tagging efficiency is estimated to be $(5.7 \pm 0.5)\%$, $(6.1 \pm 0.7)\%$ and $(6.3 \pm 0.5)\%$ for the 2015-2016, 2017 and 2018 data samples, respectively. Mistag asymmetries between B_s^0 and $\overline{B}_s^0$ decays are evaluated using $B^\pm \to J/\psi K^\pm$ decays for the OS tagging and prompt $D_s^\pm$ decays as a proxy for B_s^0 and $\overline{B}_s^0$ decays for the SS tagging, and accounted for in the subsequent signal fit.

A weighted maximum-likelihood fit [38] is simultaneously performed to the three subsamples of data recorded in 2015-2016, 2017 and 2018. The probability density function for each period is based on Eq. 1 and takes into account the effects of angular acceptance, decay-time acceptance, decay–time resolution and mistag probability. The parameter Δm_s is constrained to the measurement by the LHCb collaboration, $\Delta m_s = 17.766 \pm 0.006\ \text{ps}^{-1}$ [45]. The parameters Γ_s and $\Delta\Gamma_s$ are constrained to the recent measurements by the LHCb collaboration in $B_s^0 \to J/\psi\phi$ decays [42]: $\Gamma_s = 0.657 \pm 0.002\ \text{ps}^{-1}$ and $\Delta\Gamma_s = 0.078 \pm 0.006\ \text{ps}^{-1}$ with a correlation coefficient of -0.35.

The background-subtracted data distributions of the decay time and angular variables with projections of the polarization-independent fit are shown in Fig. 1(b-d). The fit results are summarized in Table 1, which include both statistical and systematic uncertainties. The correlation matrix is given in the Supplemental Material [46], as well as the observed time-dependent asymmetry between flavor-tagged B_s^0 and $\overline{B}_s^0$ decays.

A summary of the systematic uncertainties for the polarization-independent fit is reported in Table 2. The total systematic uncertainty on $\phi_s^{s\bar{s}s}$, which is the sum in quadrature of the different contributions, is 0.009 rad, significantly smaller than the statistical uncertainty of 0.075 rad. This is also the case for the other physics parameters.

Inaccuracies in the determination of the calibration parameters of the decay-time resolution (q_0, q_1) and the flavor tagging (p_0, p_1, p_2) lead to systematic effects on the *CP*-violation observables. These parameters are fixed in the baseline fit, and their combined statistical and systematic uncertainties are propagated to the fit parameters as systematic uncertainties. The compatibility of the calibration parameter values in control and signal channels are checked using simulated samples, and the observed differences are treated as sources of systematic uncertainties. These uncertainties are taken to be fully correlated between different data-taking periods. A bias of roughly -5 fs on the reconstructed decay time is observed in the calibration of the decay-time resolution. Neglecting this bias in the analysis of the signal decays results in negligible effects on the physics parameters.

The systematic uncertainties related to the angular acceptance comprise the uncertainties due to the limited size of the simulation sample, evaluated using a bootstrapping [47] procedure, and uncertainties associated with convergence of the

Table 1: Measured observables in the polarization-independent fit. The first uncertainties are statistical and the second systematic.

Parameter	Result
$\phi_s^{s\bar{s}ss}$ [rad]	$-0.042 \pm 0.075 \pm 0.009$
$\lvert\lambda\rvert$	$1.004 \pm 0.030 \pm 0.009$
$\lvert A_0\rvert^2$	$0.384 \pm 0.007 \pm 0.003$
$\lvert A_\perp\rvert^2$	$0.310 \pm 0.006 \pm 0.003$
$\delta_\parallel - \delta_0$ [rad]	$2.463 \pm 0.029 \pm 0.009$
$\delta_\perp - \delta_0$ [rad]	$2.769 \pm 0.105 \pm 0.011$

Table 2: Systematic uncertainties for physics parameters in the polarization-independent fit, the values are given in units of 10^{-3} (10^{-3} rad for angles).

Source	$\phi_s^{s\bar{s}ss}$	$\lvert\lambda\rvert$	$\lvert A_0\rvert^2$	$\lvert A_\perp\rvert^2$	$\delta_\parallel - \delta_0$	$\delta_\perp - \delta_0$
Time resolution	4.9	2.6	0.8	0.8	0.1	3.4
Flavor tagging	4.8	4.7	0.9	1.3	1.2	9.7
Angular acceptance	3.9	4.9	1.4	1.7	4.7	1.2
Time acceptance	2.3	1.7	0.1	0.1	5.6	0.7
Mass fit & factorization	2.2	4.4	1.9	2.3	2.3	2.5
MC truth match	1.1	0.2	0.1	0.1	0.2	0.3
Fit bias	0.8	0.7	0.9	0.3	3.6	0.7
Candidate multiplicity	0.3	0.2	0.1	0.8	0.2	0.1
Total	8.8	8.6	2.7	3.3	8.5	10.7

iterative correction procedure, estimated by comparing fit results with different numbers of iterations.

The systematic uncertainties related to the decay-time acceptance are found by varying the knot positions of the spline function to achieve similar fit quality of the decay-time distribution to that of the baseline fit. The maximum changes of the parameter estimates are assigned as systematic uncertainties.

The effects of mismodelling the signal and background mass distributions are studied by using alternative shape functions that can achieve similar fit quality to that of the baseline fit. The maximum changes of the parameter estimates are assigned as systematic uncertainties. The *sPlot* method used to subtract background in the time-dependent angular fit requires that the discriminating variable, $m(K^+K^-K^+K^-)$, is uncorrelated with the decay angles, $\vec{\Omega}$, and decay time, t. To evaluate the effects of possible correlations among these variables, the data sample is split into three subsamples according to the value of $\cos^2\theta_1 + \cos^2\theta_2$, χ or t, respectively. A fit to the $m(K^+K^-K^+K^-)$ distribution of each subsample is performed, and signal weights are calculated accordingly. The three subsamples are then recombined and a new time-dependent angular fit is performed. The maximum changes of the parameter estimates are assigned as systematic uncertainties.

The intrinsic bias from the maximum-likelihood fit with a limited sample size is evaluated by performing pseudoexperiments, which also demonstrate that the parameter

uncertainties estimated in the fit are reliable after correcting for the background dilution effect.

Various checks of the fit procedure are performed by splitting the data sample according to magnet polarity, trigger selection, tagging category, data-taking period, and multiple decay-time and B_s^0-meson $p_{\rm T}$ intervals. The effect of tightening the kaon-identification and MLP-output requirements is also studied. The fit results are compatible between different subsamples in all checks.

The polarization-independent measurements of the *CP*-violation parameters $\phi_s^{s\bar{s}s}$ and $|\lambda|$ in $B_s^0 \to \phi\phi$ decays presented here are combined with the LHCb Run 1 measurements, $\phi_s^{s\bar{s}s} = -0.17 \pm 0.15\,(\text{stat}) \pm 0.03\,(\text{syst})\,\text{rad}$ and $|\lambda| = 1.04 \pm 0.07\,(\text{stat}) \pm 0.03\,(\text{syst})$ [17] using the procedure described in Ref. [42]. In the combination, those systematic uncertainties that arise from the same origin are taken to be completely correlated between the Run 1 and Run 2 results. The combined values of the *CP*-violation parameters are $\phi_s^{s\bar{s}s} = -0.074 \pm 0.069\,\text{rad}$ and $|\lambda| = 1.009 \pm 0.030$, with a correlation coefficient of -0.02. This is the most precise measurement of *CP* violation in $B_s^0 \to \phi\phi$ decays to date, as is illustrated in Fig. 2.

A polarization-dependent fit is performed using the same data set, where the parameters $\phi_{s,i}$ and λ_i can take different values for the three polarization states. To reduce parameter correlations in the fit, the phase differences, $\phi_{s,\parallel} - \phi_{s,0}$ and $\phi_{s,\perp} - \phi_{s,0}$, and ratios, $|\lambda_\perp/\lambda_0|$ and $|\lambda_\parallel/\lambda_0|$, are used as fit parameters. The measured values are

$$\begin{aligned} \phi_{s,0} &= -0.18 \pm 0.09 \ \text{rad}\,, & |\lambda_0| &= 1.02 \pm 0.17\,, \\ \phi_{s,\parallel} - \phi_{s,0} &= \ \ 0.12 \pm 0.09 \ \text{rad}\,, & |\lambda_\perp/\lambda_0| &= 0.97 \pm 0.22\,, \\ \phi_{s,\perp} - \phi_{s,0} &= \ \ 0.17 \pm 0.09 \ \text{rad}\,, & |\lambda_\parallel/\lambda_0| &= 0.78 \pm 0.21\,, \end{aligned}$$

where the uncertainties are statistical only. No significant difference between different polarization states is observed.

In conclusion, a measurement of the polarization-independent *CP*-violation observables in $B_s^0 \to \phi\phi$ decays is performed using data collected with the LHCb detector in 2015–2018,

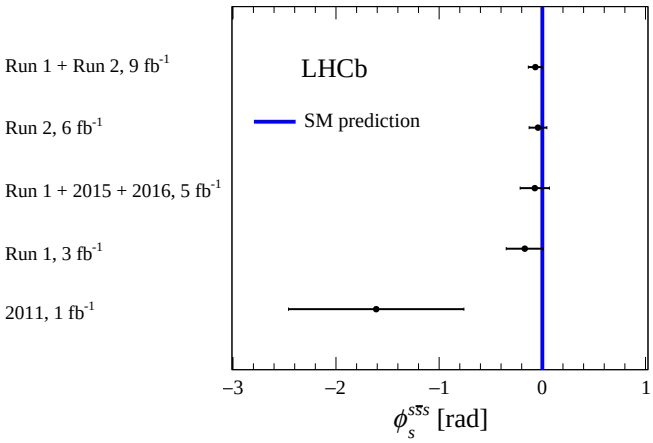

Figure 2: Comparison of $\phi_s^{s\bar{s}s}$ measurements from this and previous analyses [16–18] by the LHCb collaboration. The vertical band indicates the SM prediction [6, 7, 9].

corresponding to a total integrated luminosity of $6\,\text{fb}^{-1}$. The results are

$$\begin{aligned}\phi_s^{s\bar{s}s} &= -0.042 \pm 0.075 \pm 0.009 \text{ rad}\,,\\ |\lambda| &= \quad 1.004 \pm 0.030 \pm 0.009\,,\end{aligned}$$

where the first uncertainties are statistical and the second systematic. These results are combined with the LHCb measurements based on data taken in 2011 and 2012 to obtain $\phi_s^{s\bar{s}s} = -0.074 \pm 0.069\,\text{rad}$ and $|\lambda| = 1.009 \pm 0.030$. This is the most precise measurement of time-dependent *CP* asymmetry in the decay $B_s^0 \to \phi\phi$ and in any penguin-dominated B meson decay. The measurement is consistent with and supersedes the measurement in Ref. [18], and agrees with the SM expectation of tiny *CP* violation. For the first time, the polarization-dependent *CP*-violation parameters are measured, which show no significant difference between the three polarization states of $B_s^0 \to \phi\phi$ decays. These results can be used to constrain new physics contributions in $b \to s$ transitions [12–14].

Acknowledgements

We express our gratitude to our colleagues in the CERN accelerator departments for the excellent performance of the LHC. We thank the technical and administrative staff at the LHCb institutes. We acknowledge support from CERN and from the national agencies: CAPES, CNPq, FAPERJ and FINEP (Brazil); MOST and NSFC (China); CNRS/IN2P3 (France); BMBF, DFG and MPG (Germany); INFN (Italy); NWO (Netherlands); MNiSW and NCN (Poland); MEN/IFA (Romania); MICINN (Spain); SNSF and SER (Switzerland); NASU (Ukraine); STFC (United Kingdom); DOE NP and NSF (USA). We acknowledge the computing resources that are provided by CERN, IN2P3 (France), KIT and DESY (Germany), INFN (Italy), SURF (Netherlands), PIC (Spain), GridPP (United Kingdom), CSCS (Switzerland), IFIN-HH (Romania), CBPF (Brazil), Polish WLCG (Poland) and NERSC (USA). We are indebted to the communities behind the multiple open-source software packages on which we depend. Individual groups or members have received support from ARC and ARDC (Australia); Minciencias (Colombia); AvH Foundation (Germany); EPLANET, Marie Skłodowska-Curie Actions and ERC (European Union); A*MIDEX, ANR, IPhU and Labex P2IO, and Région Auvergne-Rhône-Alpes (France); Key Research Program of Frontier Sciences of CAS, CAS PIFI, CAS CCEPP, Fundamental Research Funds for the Central Universities, and Sci. & Tech. Program of Guangzhou (China); GVA, XuntaGal, GENCAT, Inditex and InTalent (Spain); SRC (Sweden); the Leverhulme Trust, the Royal Society and UKRI (United Kingdom).

References

[1] Belle-II collaboration, T. Abe *et al.*, *Belle II Technical Design Report*, KEK-REPORT-2010-1, (2010) arXiv:1011.0352.

[2] BaBar collaboration, B. Aubert *et al.*, *Rare B decays into states containing a J/ψ meson and a meson with $s\bar{s}$ quark content*, Phys. Rev. Lett. **91** (2003) 071801, arXiv:hep-ex/0304014.

[3] N. Cabibbo, *Unitary symmetry and leptonic decays*, Phys. Rev. Lett. **10** (1963) 531.

[4] M. Kobayashi and T. Maskawa, *CP-violation in the renormalizable theory of weak interaction*, Prog. Theor. Phys. **49** (1973) 652.

[5] P. Huet and E. Sather, *Electroweak baryogenesis and standard model CP violation*, Phys. Rev. **D51** (1995) 379, arXiv:hep-ph/9404302.

[6] M. Raidal, *CP asymmetry in $B \to \phi K_s$ decays in left-right models and its implications on B_s decays*, Phys. Rev. Lett. **89** (2002) 231803, arXiv:hep-ph/0208091.

[7] M. Beneke, J. Rohrer, and D. Yang, *Branching fractions, polarisation and asymmetries of $B \to VV$ decays*, Nucl. Phys. **B774** (2007) 64, arXiv:hep-ph/0612290.

[8] M. Bartsch, G. Buchalla, and C. Kraus, *$B \to V_L V_L$ decays at next-to-leading order in QCD*, arXiv:0810.0249.

[9] H.-Y. Cheng and C.-K. Chua, *QCD factorization for charmless hadronic B_s decays revisited*, Phys. Rev. **D80** (2009) 114026, arXiv:0910.5237.

[10] C. Wang, S.-H. Zhou, Y. Li, and C.-D. Lu, *Global analysis of charmless B decays into two vector mesons in soft-collinear effective theory*, Phys. Rev. **D96** (2017) 073004, arXiv:1708.04861.

[11] D.-C. Yan, X. Liu, and Z.-J. Xiao, *Anatomy of $B_s \to VV$ decays and effects of next-to-leading order contributions in the perturbative QCD factorization approach*, Nucl. Phys. **B935** (2018) 17, arXiv:1807.00606.

[12] D. Zhang, Z.-j. Xiao, and C. S. Li, *Branching ratios and CP violating asymmetries of $B_s \to h_1 h_2$ decays in the general two Higgs doublet model*, Phys. Rev. **D64** (2001) 014014, arXiv:hep-ph/0012063.

[13] A. Datta, M. Duraisamy, and D. London, *New physics in $b \to s$ transitions and the $B^0_{d,s} \to V_1 V_2$ angular analysis*, Phys. Rev. **D86** (2012) 076011, arXiv:1207.4495.

[14] B. Bhattacharya, A. Datta, M. Duraisamy, and D. London, *Searching for new physics with $\bar{b} \to \bar{s}$ $B^0_s \to V_1 V_2$ penguin decays*, Phys. Rev. **D88** (2013) 016007, arXiv:1306.1911.

[15] T. Kapoor and E. Kou, *New physics search via CP observables in $B^0_s \to \phi\phi$ decays with left- and right-handed Chromomagnetic operators*, arXiv:2303.04494.

[16] LHCb collaboration, R. Aaij *et al.*, *First measurement of the CP-violating phase in $B^0_s \to \phi\phi$ decays*, Phys. Rev. Lett. **110** (2013) 241802, arXiv:1303.7125.

[17] LHCb collaboration, R. Aaij *et al.*, *Measurement of CP violation in $B^0_s \to \phi\phi$ decays*, Phys. Rev. **D90** (2014) 052011, arXiv:1407.2222.

[18] LHCb collaboration, R. Aaij *et al.*, *Measurement of CP violation in the $B^0_s \to \phi\phi$ decay and search for the $B^0 \to \phi\phi$ decay*, JHEP **12** (2019) 155, arXiv:1907.10003.

[19] LHCb collaboration, A. A. Alves Jr. *et al.*, *The LHCb detector at the LHC*, JINST **3** (2008) S08005.

[20] LHCb collaboration, R. Aaij *et al.*, *LHCb detector performance*, Int. J. Mod. Phys. **A30** (2015) 1530022, arXiv:1412.6352.

[21] T. Sjöstrand, S. Mrenna, and P. Skands, *A brief introduction to PYTHIA 8.1*, Comput. Phys. Commun. **178** (2008) 852, arXiv:0710.3820.

[22] T. Sjöstrand, S. Mrenna, and P. Skands, *PYTHIA 6.4 physics and manual*, JHEP **05** (2006) 026, arXiv:hep-ph/0603175.

[23] I. Belyaev *et al.*, *Handling of the generation of primary events in Gauss, the LHCb simulation framework*, J. Phys. Conf. Ser. **331** (2011) 032047.

[24] Geant4 collaboration, S. Agostinelli *et al.*, *Geant4: A simulation toolkit*, Nucl. Instrum. Meth. **A506** (2003) 250.

[25] Geant4 collaboration, J. Allison *et al.*, *Geant4 developments and applications*, IEEE Trans. Nucl. Sci. **53** (2006) 270.

[26] M. Clemencic *et al.*, *The LHCb simulation application, Gauss: design, evolution and experience*, J. Phys. Conf. Ser. **331** (2011) 032023.

[27] N. Davidson, T. Przedzinski, and Z. Was, *PHOTOS interface in C++: Technical and physics documentation*, Comp. Phys. Comm. **199** (2016) 86, arXiv:1011.0937.

[28] R. Aaij *et al.*, *The LHCb trigger and its performance in 2011*, Journal of Instrumentation **8** (2013) P04022.

[29] T. Likhomanenko *et al.*, *LHCb topological trigger reoptimization*, J. Phys. Conf. Ser. **664** (2015) 082025.

[30] Particle Data Group, R. L. Workman *et al.*, *Review of particle physics*, Prog. Theor. Exp. Phys. **2022** (2022) 083C01.

[31] H. Voss, A. Hoecker, J. Stelzer, and F. Tegenfeldt, *TMVA - Toolkit for Multivariate Data Analysis with ROOT*, PoS **ACAT** (2007) 040.

[32] T. Hastie, J. Friedman, and R. Tibshirani, in *Model inference and averaging*, pp. 225–256, Springer New York, New York, NY, 2001.

[33] A. Blum, A. T. Kalai, and J. Langford, *Beating the hold-out: bounds for k-fold and progressive cross-validation*, in *Annual Conference Computational Learning Theory*, 1999.

[34] T. Skwarnicki, *A study of the radiative cascade transitions between the Upsilon-prime and Upsilon resonances*, PhD thesis, Institute of Nuclear Physics, Krakow, 1986, DESY-F31-86-02.

[35] C. Bishop, *Pattern recognition and machine learning (Information Science and Statistics)*, Springer-Verlag New York, Inc., Secaucus, 2007.

[36] G. A. Cowan, D. C. Craik, and M. D. Needham, *Rapidsim: An application for the fast simulation of heavy-quark hadron decays*, Computer Physics Communications **214** (2017) 239.

[37] M. Pivk and F. R. Le Diberder, *sPlot: A statistical tool to unfold data distributions*, Nucl. Instrum. Meth. **A555** (2005) 356, arXiv:physics/0402083.

[38] Y. Xie, *sFit: a method for background subtraction in maximum likelihood fit*, arXiv:0905.0724.

[39] Heavy Flavor Averaging Group, Y. Amhis *et al.*, *Averages of b-hadron, c-hadron, and τ-lepton properties as of 2018*, Eur. Phys. J. **C81** (2021) 226, arXiv:1909.12524, updated results and plots available at https://hflav.web.cern.ch.

[40] LHCb collaboration, R. Aaij *et al.*, *Measurement of CP violation and the B_s^0 meson decay width difference with $B_s^0 \to J/\psi K^+K^-$ and $B_s^0 \to J/\psi\pi^+\pi^-$ decays*, Phys. Rev. **D87** (2013) 112010, arXiv:1304.2600.

[41] T. M. Karbach, G. Raven, and M. Schiller, *Decay time integrals in neutral meson mixing and their efficient evaluation*, arXiv:1407.0748.

[42] LHCb collaboration, R. Aaij *et al.*, *Updated measurement of time-dependent CP-violating observables in $B_s^0 \to J/\psi K^+K^-$ decays*, Eur. Phys. J. **C79** (2019) 706, Erratum ibid. **C80** (2020) 601, arXiv:1906.08356.

[43] LHCb collaboration, R. Aaij *et al.*, *Opposite-side flavour tagging of B mesons at the LHCb experiment*, Eur. Phys. J. **C72** (2012) 2022, arXiv:1202.4979.

[44] LHCb collaboration, R. Aaij *et al.*, *A new algorithm for identifying the flavour of B_s^0 mesons at LHCb*, JINST **11** (2016) P05010, arXiv:1602.07252.

[45] LHCb collaboration, R. Aaij *et al.*, *Precise determination of the $B_s^0 - \bar{B}_s^0$ oscillation frequency*, Nature Physics **18** (2022) 1, arXiv:2104.04421.

[46] *See supplementary material at [link inserted by publisher] for the correlation matrix of the measured observables and a plot of the observed time-dependent asymmetries between B_s^0 and $\overline{B}_s^0$ decays.*

[47] B. Efron and R. Tibshirani, *Bootstrap methods for standard errors, confidence intervals, and other measures of statistical accuracy*, Statistical Science **1** (1986) 54.

Supplemental material

Table 3 shows the correlation matrix for the measured observables using LHCb Run 2 data. The observed asymmetry between flavor-tagged B_s^0 and $\overline{B}_s^0$ decays, as a function of decay time, is shown in Fig. 3.

Table 3: Correlation matrix in the polarization-independent fit result. Both statistical and systematic uncertainties are accounted for.

	$\phi_s^{s\bar{s}s}$	$\lvert\lambda\rvert$	$\lvert A_0\rvert^2$	$\lvert A_\perp\rvert^2$	$\delta_\parallel - \delta_0$	$\delta_\perp - \delta_0$
$\phi_s^{s\bar{s}s}$	1	-0.037	-0.005	0.058	0.013	-0.005
$\lvert\lambda\rvert$		1	0.033	0.018	-0.008	-0.006
$\lvert A_0\rvert^2$			1	-0.342	-0.007	0.064
$\lvert A_\perp\rvert^2$				1	0.140	0.088
$\delta_\parallel - \delta_0$					1	0.179
$\delta_\perp - \delta_0$						1

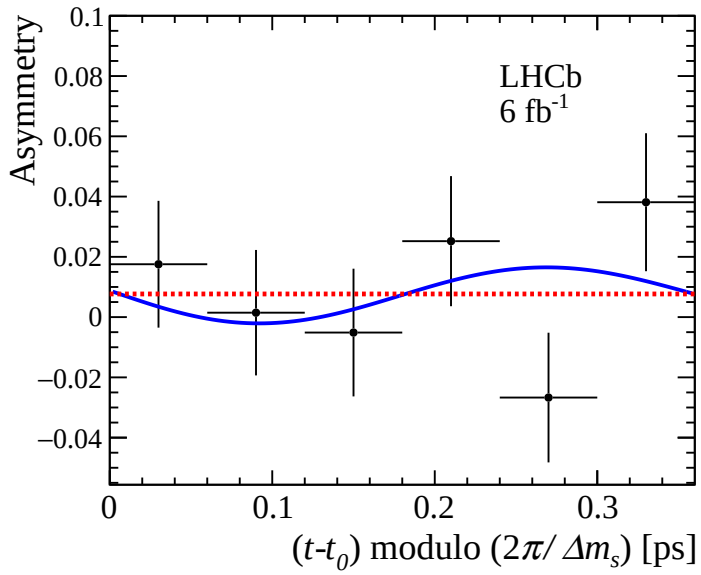

Figure 3: Observed rate asymmetry between decays of flavor-tagged B_s^0 or $\bar{B}_s^0$ mesons to a $\phi\phi$ pair, as a function of decay time t, folded into a single B_s^0 oscillation period (black points), overlaid with the projection of the polarization-independent fit result (blue solid line). The minimum requirement on the decay time of the B_s^0 candidates, t_0, is 0.3 ps. The red dashed line corresponds to the hypothesis of *CP* symmetry. Its non-zero asymmetry is a combined effect of the B_s^0 production asymmetry and tagging efficiency asymmetry. The p value of the *CP* symmetry hypothesis is 0.684, evaluated using the difference of the log-likelihood value of the fit with polarization-independent *CP*-violation parameters and the fit that assumes *CP* symmetry, $\Delta \ln L = 0.38$.

LHCb collaboration

R. Aaij[32], A.S.W. Abdelmotteleb[51], C. Abellan Beteta[45], F. Abudinén[51], T. Ackernley[55], B. Adeva[41], M. Adinolfi[49], P. Adlarson[77], H. Afsharnia[9], C. Agapopoulou[43], C.A. Aidala[78], Z. Ajaltouni[9], S. Akar[60], K. Akiba[32], P. Albicocco[23], J. Albrecht[15], F. Alessio[43], M. Alexander[54], A. Alfonso Albero[40], Z. Aliouche[57], P. Alvarez Cartelle[50], R. Amalric[13], S. Amato[2], J.L. Amey[49], Y. Amhis[11,43], L. An[5], L. Anderlini[22], M. Andersson[45], A. Andreianov[38], M. Andreotti[21], D. Andreou[63], D. Ao[6], F. Archilli[31,t], A. Artamonov[38], M. Artuso[63], E. Aslanides[10], M. Atzeni[45], B. Audurier[12], I.B Bachiller Perea[8], S. Bachmann[17], M. Bachmayer[44], J.J. Back[51], A. Bailly-reyre[13], P. Baladron Rodriguez[41], V. Balagura[12], W. Baldini[21,43], J. Baptista de Souza Leite[1], M. Barbetti[22,j], R.J. Barlow[57], S. Barsuk[11], W. Barter[53], M. Bartolini[50], F. Baryshnikov[38], J.M. Basels[14], G. Bassi[29], V. Batozskaya[36], B. Batsukh[4], A. Battig[15], A. Bay[44], A. Beck[51], M. Becker[15], F. Bedeschi[29], I.B. Bediaga[1], A. Beiter[63], S. Belin[41], V. Bellee[45], K. Belous[38], I. Belov[38], I. Belyaev[38], G. Benane[10], G. Bencivenni[23], E. Ben-Haim[13], A. Berezhnoy[38], R. Bernet[45], S. Bernet Andres[39], D. Berninghoff[17], H.C. Bernstein[63], C. Bertella[57], A. Bertolin[28], C. Betancourt[45], F. Betti[43], Ia. Bezshyiko[45], J. Bhom[35], L. Bian[69], M.S. Bieker[15], N.V. Biesuz[21], P. Billoir[13], A. Biolchini[32], M. Birch[56], F.C.R. Bishop[50], A. Bitadze[57], A. Bizzeti, M.P. Blago[50], T. Blake[51], F. Blanc[44], J.E. Blank[15], S. Blusk[63], D. Bobulska[54], V.B Bocharnikov[38], J.A. Boelhauve[15], O. Boente Garcia[12], T. Boettcher[60], A. Boldyrev[38], C.S. Bolognani[75], R. Bolzonella[21,i], N. Bondar[38], F. Borgato[28], S. Borghi[57], M. Borsato[17], J.T. Borsuk[35], S.A. Bouchiba[44], T.J.V. Bowcock[55], A. Boyer[43], C. Bozzi[21], M.J. Bradley[56], S. Braun[61], A. Brea Rodriguez[41], N. Breer[15], J. Brodzicka[35], A. Brossa Gonzalo[41], J. Brown[55], D. Brundu[27], A. Buonaura[45], L. Buonincontri[28], A.T. Burke[57], C. Burr[43], A. Bursche[67], A. Butkevich[38], J.S. Butter[32], J. Buytaert[43], W. Byczynski[43], S. Cadeddu[27], H. Cai[69], R. Calabrese[21,i], L. Calefice[15], S. Cali[23], M. Calvi[26,m], M. Calvo Gomez[39], P. Campana[23], D.H. Campora Perez[75], A.F. Campoverde Quezada[6], S. Capelli[26,m], L. Capriotti[21], A. Carbone[20,g], R. Cardinale[24,k], A. Cardini[27], P. Carniti[26,m], L. Carus[14], A. Casais Vidal[41], R. Caspary[17], G. Casse[55], M. Cattaneo[43], G. Cavallero[21], V. Cavallini[21,i], S. Celani[44], J. Cerasoli[10], D. Cervenkov[58], A.J. Chadwick[55], I.C Chahrour[78], M.G. Chapman[49], M. Charles[13], Ph. Charpentier[43], C.A. Chavez Barajas[55], M. Chefdeville[8], C. Chen[10], S. Chen[4], A. Chernov[35], S. Chernyshenko[47], V. Chobanova[41], S. Cholak[44], M. Chrzaszcz[35], A. Chubykin[38], V. Chulikov[38], P. Ciambrone[23], M.F. Cicala[51], X. Cid Vidal[41], G. Ciezarek[43], P. Cifra[43], P.E.L. Clarke[53], M. Clemencic[43], H.V. Cliff[50], J. Closier[43], J.L. Cobbledick[57], V. Coco[43], J. Cogan[10], E. Cogneras[9], L. Cojocariu[37], P. Collins[43], T. Colombo[43], L. Congedo[19], A. Contu[27], N. Cooke[48], I. Corredoira [41], G. Corti[43], B. Couturier[43], D.C. Craik[45], M. Cruz Torres[1,e], R. Currie[53], C.L. Da Silva[62], S. Dadabaev[38], L. Dai[66], X. Dai[5], E. Dall'Occo[15], J. Dalseno[41], C. D'Ambrosio[43], J. Daniel[9], A. Danilina[38], P. d'Argent[19], J.E. Davies[57], A. Davis[57], O. De Aguiar Francisco[57], J. de Boer[43], K. De Bruyn[74], S. De Capua[57], M. De Cian[44], U. De Freitas Carneiro Da Graca[1], E. De Lucia[23], J.M. De Miranda[1], L. De Paula[2], M. De Serio[19,f], D. De Simone[45], P. De Simone[23], F. De Vellis[15], J.A. de Vries[75], C.T. Dean[62], F. Debernardis[19,f], D. Decamp[8], V. Dedu[10], L. Del Buono[13], B. Delaney[59], H.-P. Dembinski[15], V. Denysenko[45], O. Deschamps[9], F. Dettori[27], B. Dey[72], P. Di Nezza[23], I. Diachkov[38],

S. Didenko[38], L. Dieste Maronas[41], S. Ding[63], V. Dobishuk[47], A. Dolmatov[38], C. Dong[3], A.M. Donohoe[18], F. Dordei[27], A.C. dos Reis[1], L. Douglas[54], A.G. Downes[8], P. Duda[76], M.W. Dudek[35], L. Dufour[43], V. Duk[73], P. Durante[43], M. M. Duras[76], J.M. Durham[62], D. Dutta[57], A. Dziurda[35], A. Dzyuba[38], S. Easo[52], U. Egede[64], A. Egorychev[38], V. Egorychev[38], C. Eirea Orro[41], S. Eisenhardt[53], E. Ejopu[57], S. Ek-In[44], L. Eklund[77], M.E Elashri[60], J. Ellbracht[15], S. Ely[56], A. Ene[37], E. Epple[60], S. Escher[14], J. Eschle[45], S. Esen[45], T. Evans[57], F. Fabiano[27], L.N. Falcao[1], Y. Fan[6], B. Fang[11,69], L. Fantini[73,p], M. Faria[44], S. Farry[55], D. Fazzini[26,m], L.F Felkowski[76], M. Feo[43], M. Fernandez Gomez[41], A.D. Fernez[61], F. Ferrari[20], L. Ferreira Lopes[44], F. Ferreira Rodrigues[2], S. Ferreres Sole[32], M. Ferrillo[45], M. Ferro-Luzzi[43], S. Filippov[38], R.A. Fini[19], M. Fiorini[21,i], M. Firlej[34], K.M. Fischer[58], D.S. Fitzgerald[78], C. Fitzpatrick[57], T. Fiutowski[34], F. Fleuret[12], M. Fontana[20], F. Fontanelli[24,k], R. Forty[43], D. Foulds-Holt[50], V. Franco Lima[55], M. Franco Sevilla[61], M. Frank[43], E. Franzoso[21,i], G. Frau[17], C. Frei[43], D.A. Friday[57], L.F Frontini[25,l], J. Fu[6], Q. Fuehring[15], T. Fulghesu[13], E. Gabriel[32], G. Galati[19,f], M.D. Galati[32], A. Gallas Torreira[41], D. Galli[20,g], S. Gambetta[53,43], M. Gandelman[2], P. Gandini[25], H.G Gao[6], R. Gao[58], Y. Gao[7], Y. Gao[5], M. Garau[27], L.M. Garcia Martin[51], P. Garcia Moreno[40], J. García Pardiñas[43], B. Garcia Plana[41], F.A. Garcia Rosales[12], L. Garrido[40], C. Gaspar[43], R.E. Geertsema[32], D. Gerick[17], L.L. Gerken[15], E. Gersabeck[57], M. Gersabeck[57], T. Gershon[51], L. Giambastiani[28], V. Gibson[50], H.K. Giemza[36], A.L. Gilman[58], M. Giovannetti[23], A. Gioventù[41], P. Gironella Gironell[40], C. Giugliano[21,i], M.A. Giza[35], K. Gizdov[53], E.L. Gkougkousis[43], V.V. Gligorov[13], C. Göbel[65], E. Golobardes[39], D. Golubkov[38], A. Golutvin[56,38], A. Gomes[1,a], S. Gomez Fernandez[40], F. Goncalves Abrantes[58], M. Goncerz[35], G. Gong[3], I.V. Gorelov[38], C. Gotti[26], J.P. Grabowski[71], T. Grammatico[13], L.A. Granado Cardoso[43], E. Graugés[40], E. Graverini[44], G. Graziani, A. T. Grecu[37], L.M. Greeven[32], N.A. Grieser[60], L. Grillo[54], S. Gromov[38], C. Gu[3], M. Guarise[21], M. Guittiere[11], V. Guliaeva[38], P. A. Günther[17], A.K. Guseinov[38], E. Gushchin[38], Y. Guz[5,38,43], T. Gys[43], T. Hadavizadeh[64], C. Hadjivasiliou[61], G. Haefeli[44], C. Haen[43], J. Haimberger[43], S.C. Haines[50], T. Halewood-leagas[55], M.M. Halvorsen[43], P.M. Hamilton[61], J. Hammerich[55], Q. Han[7], X. Han[17], S. Hansmann-Menzemer[17], N. Harnew[58], T. Harrison[55], C. Hasse[43], M. Hatch[43], J. He[6,c], K. Heijhoff[32], F.H Hemmer[43], C. Henderson[60], R.D.L. Henderson[64,51], A.M. Hennequin[59], K. Hennessy[55], L. Henry[43], J.H Herd[56], J. Heuel[14], A. Hicheur[2], D. Hill[44], M. Hilton[57], S.E. Hollitt[15], J. Horswill[57], R. Hou[7], Y. Hou[8], J. Hu[17], J. Hu[67], W. Hu[5], X. Hu[3], W. Huang[6], X. Huang[69], W. Hulsbergen[32], R.J. Hunter[51], M. Hushchyn[38], D. Hutchcroft[55], P. Ibis[15], M. Idzik[34], D. Ilin[38], P. Ilten[60], A. Inglessi[38], A. Iniukhin[38], A. Ishteev[38], K. Ivshin[38], R. Jacobsson[43], H. Jage[14], S.J. Jaimes Elles[42], S. Jakobsen[43], E. Jans[32], B.K. Jashal[42], A. Jawahery[61], V. Jevtic[15], E. Jiang[61], X. Jiang[4,6], Y. Jiang[6], M. John[58], D. Johnson[59], C.R. Jones[50], T.P. Jones[51], S.J Joshi[36], B. Jost[43], N. Jurik[43], I. Juszczak[35], S. Kandybei[46], Y. Kang[3], M. Karacson[43], D. Karpenkov[38], M. Karpov[38], J.W. Kautz[60], F. Keizer[43], D.M. Keller[63], M. Kenzie[51], T. Ketel[32], B. Khanji[63], A. Kharisova[38], S. Kholodenko[38], G. Khreich[11], T. Kirn[14], V.S. Kirsebom[44], O. Kitouni[59], S. Klaver[33], N. Kleijne[29,q], K. Klimaszewski[36], M.R. Kmiec[36], S. Koliiev[47], L. Kolk[15], A. Kondybayeva[38], A. Konoplyannikov[38], P. Kopciewicz[34], R. Kopecna[17], P. Koppenburg[32], M. Korolev[38], I. Kostiuk[32], O. Kot[47], S. Kotriakhova,

A. Kozachuk[38], P. Kravchenko[38], L. Kravchuk[38], M. Kreps[51], S. Kretzschmar[14], P. Krokovny[38], W. Krupa[34], W. Krzemien[36], J. Kubat[17], S. Kubis[76], W. Kucewicz[35], M. Kucharczyk[35], V. Kudryavtsev[38], E.K Kulikova[38], A. Kupsc[77], D. Lacarrere[43], G. Lafferty[57], A. Lai[27], A. Lampis[27], D. Lancierini[45], C. Landesa Gomez[41], J.J. Lane[57], R. Lane[49], C. Langenbruch[14], J. Langer[15], O. Lantwin[38], T. Latham[51], F. Lazzari[29,r], C. Lazzeroni[48], R. Le Gac[10], S.H. Lee[78], R. Lefèvre[9], A. Leflat[38], S. Legotin[38], O. Leroy[10], T. Lesiak[35], B. Leverington[17], A. Li[3], H. Li[67], K. Li[7], P. Li[43], P.-R. Li[68], S. Li[7], T. Li[4], T. Li[67], Y. Li[4], Z. Li[63], X. Liang[63], C. Lin[6], T. Lin[52], R. Lindner[43], V. Lisovskyi[15], R. Litvinov[27], G. Liu[67], H. Liu[6], K. Liu[68], Q. Liu[6], S. Liu[4,6], A. Lobo Salvia[40], A. Loi[27], R. Lollini[73], J. Lomba Castro[41], I. Longstaff[54], J.H. Lopes[2], A. Lopez Huertas[40], S. López Soliño[41], G.H. Lovell[50], Y. Lu[4,b], C. Lucarelli[22,j], D. Lucchesi[28,o], S. Luchuk[38], M. Lucio Martinez[75], V. Lukashenko[32,47], Y. Luo[3], A. Lupato[57], E. Luppi[21,i], K. Lynch[18], X.-R. Lyu[6], R. Ma[6], S. Maccolini[15], F. Machefert[11], F. Maciuc[37], I. Mackay[58], V. Macko[44], L.R. Madhan Mohan[50], A. Maevskiy[38], D. Maisuzenko[38], M.W. Majewski[34], J.J. Malczewski[35], S. Malde[58], B. Malecki[35,43], A. Malinin[38], T. Maltsev[38], G. Manca[27,h], G. Mancinelli[10], C. Mancuso[11,25,l], R. Manera Escalero[40], D. Manuzzi[20], C.A. Manzari[45], D. Marangotto[25,l], J.M. Maratas[9,v], J.F. Marchand[8], U. Marconi[20], S. Mariani[43], C. Marin Benito[40], J. Marks[17], A.M. Marshall[49], P.J. Marshall[55], G. Martelli[73,p], G. Martellotti[30], L. Martinazzoli[43,m], M. Martinelli[26,m], D. Martinez Santos[41], F. Martinez Vidal[42], A. Massafferri[1], M. Materok[14], R. Matev[43], A. Mathad[45], V. Matiunin[38], C. Matteuzzi[63,26], K.R. Mattioli[12], A. Mauri[56], E. Maurice[12], J. Mauricio[40], M. Mazurek[43], M. McCann[56], L. Mcconnell[18], T.H. McGrath[57], N.T. McHugh[54], A. McNab[57], R. McNulty[18], B. Meadows[60], G. Meier[15], D. Melnychuk[36], S. Meloni[26,m], M. Merk[32,75], A. Merli[25], L. Meyer Garcia[2], D. Miao[4,6], H. Miao[6], M. Mikhasenko[71,d], D.A. Milanes[70], M. Milovanovic[43], M.-N. Minard[8,†], A. Minotti[26,m], E. Minucci[63], T. Miralles[9], S.E. Mitchell[53], B. Mitreska[15], D.S. Mitzel[15], A. Modak[52], A. Mödden [15], R.A. Mohammed[58], R.D. Moise[14], S. Mokhnenko[38], T. Mombächer[41], M. Monk[51,64], I.A. Monroy[70], S. Monteil[9], G. Morello[23], M.J. Morello[29,q], M.P. Morgenthaler[17], J. Moron[34], A.B. Morris[43], A.G. Morris[10], R. Mountain[63], H. Mu[3], E. Muhammad[51], F. Muheim[53], M. Mulder[74], K. Müller[45], D. Murray[57], R. Murta[56], P. Muzzetto[27], P. Naik[49], T. Nakada[44], R. Nandakumar[52], T. Nanut[43], I. Nasteva[2], M. Needham[53], N. Neri[25,l], S. Neubert[71], N. Neufeld[43], P. Neustroev[38], R. Newcombe[56], J. Nicolini[15,11], D. Nicotra[75], E.M. Niel[44], S. Nieswand[14], N. Nikitin[38], N.S. Nolte[59], C. Normand[8], J. Novoa Fernandez[41], G.N Nowak[60], C. Nunez[78], A. Oblakowska-Mucha[34], V. Obraztsov[38], T. Oeser[14], S. Okamura[21,i], R. Oldeman[27,h], F. Oliva[53], C.J.G. Onderwater[74], R.H. O'Neil[53], J.M. Otalora Goicochea[2], T. Ovsiannikova[38], P. Owen[45], A. Oyanguren[42], O. Ozcelik[53], K.O. Padeken[71], B. Pagare[51], P.R. Pais[43], T. Pajero[58], A. Palano[19], M. Palutan[23], G. Panshin[38], L. Paolucci[51], A. Papanestis[52], M. Pappagallo[19,f], L.L. Pappalardo[21,i], C. Pappenheimer[60], W. Parker[61], C. Parkes[57], B. Passalacqua[21], G. Passaleva[22], A. Pastore[19], M. Patel[56], C. Patrignani[20,g], C.J. Pawley[75], A. Pellegrino[32], M. Pepe Altarelli[43], S. Perazzini[20], D. Pereima[38], A. Pereiro Castro[41], P. Perret[9], K. Petridis[49], A. Petrolini[24,k], S. Petrucci[53], M. Petruzzo[25], H. Pham[63], A. Philippov[38], R. Piandani[6], L. Pica[29,q], M. Piccini[73], B. Pietrzyk[8], G. Pietrzyk[11], D. Pinci[30], F. Pisani[43], M. Pizzichemi[26,m,43], V. Placinta[37], J. Plews[48], M. Plo Casasus[41],

F. Polci[13,43], M. Poli Lener[23], A. Poluektov[10], N. Polukhina[38], I. Polyakov[43], E. Polycarpo[2], S. Ponce[43], D. Popov[6,43], S. Poslavskii[38], K. Prasanth[35], L. Promberger[17], C. Prouve[41], V. Pugatch[47], V. Puill[11], G. Punzi[29,r], H.R. Qi[3], W. Qian[6], N. Qin[3], S. Qu[3], R. Quagliani[44], N.V. Raab[18], B. Rachwal[34], J.H. Rademacker[49], R. Rajagopalan[63], M. Rama[29], M. Ramos Pernas[51], M.S. Rangel[2], F. Ratnikov[38], G. Raven[33], M. Rebollo De Miguel[42], F. Redi[43], J. Reich[49], F. Reiss[57], Z. Ren[3], P.K. Resmi[58], R. Ribatti[29,q], A.M. Ricci[27], S. Ricciardi[52], K. Richardson[59], M. Richardson-Slipper[53], K. Rinnert[55], P. Robbe[11], G. Robertson[53], E. Rodrigues[55,43], E. Rodriguez Fernandez[41], J.A. Rodriguez Lopez[70], E. Rodriguez Rodriguez[41], D.L. Rolf[43], A. Rollings[58], P. Roloff[43], V. Romanovskiy[38], M. Romero Lamas[41], A. Romero Vidal[41], M. Rotondo[23], M.S. Rudolph[63], T. Ruf[43], R.A. Ruiz Fernandez[41], J. Ruiz Vidal[42], A. Ryzhikov[38], J. Ryzka[34], J.J. Saborido Silva[41], N. Sagidova[38], N. Sahoo[48], B. Saitta[27,h], M. Salomoni[43], C. Sanchez Gras[32], I. Sanderswood[42], R. Santacesaria[30], C. Santamarina Rios[41], M. Santimaria[23], L. Santoro [1], E. Santovetti[31], D. Saranin[38], G. Sarpis[53], M. Sarpis[71], A. Sarti[30], C. Satriano[30,s], A. Satta[31], M. Saur[5], D. Savrina[38], H. Sazak[9], L.G. Scantlebury Smead[58], A. Scarabotto[13], S. Schael[14], S. Scherl[55], A. M. Schertz[72], M. Schiller[54], H. Schindler[43], M. Schmelling[16], B. Schmidt[43], S. Schmitt[14], O. Schneider[44], A. Schopper[43], M. Schubiger[32], N. Schulte[15], S. Schulte[44], M.H. Schune[11], R. Schwemmer[43], G. Schwering[14], B. Sciascia[23], A. Sciuccati[43], S. Sellam[41], A. Semennikov[38], M. Senghi Soares[33], A. Sergi[24,k], N. Serra[45], L. Sestini[28], A. Seuthe[15], Y. Shang[5], D.M. Shangase[78], M. Shapkin[38], I. Shchemerov[38], L. Shchutska[44], T. Shears[55], L. Shekhtman[38], Z. Shen[5], S. Sheng[4,6], V. Shevchenko[38], B. Shi[6], E.B. Shields[26,m], Y. Shimizu[11], E. Shmanin[38], R. Shorkin[38], J.D. Shupperd[63], B.G. Siddi[21,i], R. Silva Coutinho[63], G. Simi[28], S. Simone[19,f], M. Singla[64], N. Skidmore[57], R. Skuza[17], T. Skwarnicki[63], M.W. Slater[48], J.C. Smallwood[58], J.G. Smeaton[50], E. Smith[45], K. Smith[62], M. Smith[56], A. Snoch[32], L. Soares Lavra[9], M.D. Sokoloff[60], F.J.P. Soler[54], A. Solomin[38,49], A. Solovev[38], I. Solovyev[38], R. Song[64], F.L. Souza De Almeida[2], B. Souza De Paula[2], E. Spadaro Norella[25,l], E. Spedicato[20], J.G. Speer[15], E. Spiridenkov[38], P. Spradlin[54], V. Sriskaran[43], F. Stagni[43], M. Stahl[43], S. Stahl[43], S. Stanislaus[58], E.N. Stein[43], O. Steinkamp[45], O. Stenyakin[38], H. Stevens[15], D. Strekalina[38], Y.S Su[6], F. Suljik[58], J. Sun[27], L. Sun[69], Y. Sun[61], P.N. Swallow[48], K. Swientek[34], A. Szabelski[36], T. Szumlak[34], M. Szymanski[43], Y. Tan[3], S. Taneja[57], M.D. Tat[58], A. Terentev[45], F. Teubert[43], E. Thomas[43], D.J.D. Thompson[48], H. Tilquin[56], V. Tisserand[9], S. T'Jampens[8], M. Tobin[4], L. Tomassetti[21,i], G. Tonani[25,l], X. Tong[5], D. Torres Machado[1], L. Toscano[15], D.Y. Tou[3], C. Trippl[44], G. Tuci[17], N. Tuning[32], A. Ukleja[36], D.J. Unverzagt[17], A. Usachov[33], A. Ustyuzhanin[38], U. Uwer[17], V. Vagnoni[20], A. Valassi[43], G. Valenti[20], N. Valls Canudas[39], M. Van Dijk[44], H. Van Hecke[62], E. van Herwijnen[56], C.B. Van Hulse[41,w], M. van Veghel[32], R. Vazquez Gomez[40], P. Vazquez Regueiro[41], C. Vázquez Sierra[41], S. Vecchi[21], J.J. Velthuis[49], M. Veltri[22,u], A. Venkateswaran[44], M. Vesterinen[51], D. Vieira[60], M. Vieites Diaz[44], X. Vilasis-Cardona[39], E. Vilella Figueras[55], A. Villa[20], P. Vincent[13], F.C. Volle[11], D. vom Bruch[10], V. Vorobyev[38], N. Voropaev[38], K. Vos[75], C. Vrahas[53], J. Walsh[29], E.J. Walton[64], G. Wan[5], C. Wang[17], G. Wang[7], J. Wang[5], J. Wang[4], J. Wang[3], J. Wang[69], M. Wang[25], R. Wang[49], X. Wang[67], Y. Wang[7], Z. Wang[45], Z. Wang[3], Z. Wang[6], J.A. Ward[51,64], N.K. Watson[48], D. Websdale[56], Y. Wei[5], B.D.C. Westhenry[49], D.J. White[57], M. Whitehead[54], A.R. Wiederhold[51],

D. Wiedner[15], G. Wilkinson[58], M.K. Wilkinson[60], I. Williams[50], M. Williams[59], M.R.J. Williams[53], R. Williams[50], F.F. Wilson[52], W. Wislicki[36], M. Witek[35], L. Witola[17], C.P. Wong[62], G. Wormser[11], S.A. Wotton[50], H. Wu[63], J. Wu[7], Y. Wu[5], K. Wyllie[43], Z. Xiang[6], Y. Xie[7], A. Xu[5], J. Xu[6], L. Xu[3], L. Xu[3], M. Xu[51], Q. Xu[6], Z. Xu[9], Z. Xu[6], Z. Xu[4], D. Yang[3], S. Yang[6], X. Yang[5], Y. Yang[6], Z. Yang[5], Z. Yang[61], V. Yeroshenko[11], H. Yeung[57], H. Yin[7], J. Yu[66], X. Yuan[63], E. Zaffaroni[44], M. Zavertyaev[16], M. Zdybal[35], M. Zeng[3], C. Zhang[5], D. Zhang[7], J.Z Zhang[6], L. Zhang[3], S. Zhang[66], S. Zhang[5], Y. Zhang[5], Y. Zhang[58], Y. Zhao[17], A. Zharkova[38], A. Zhelezov[17], Y. Zheng[6], T. Zhou[5], X. Zhou[7], Y. Zhou[6], V. Zhovkovska[11], X. Zhu[3], X. Zhu[7], Z. Zhu[6], V. Zhukov[14,38], J. Zhuo[42], Q. Zou[4,6], S. Zucchelli[20,g], D. Zuliani[28], G. Zunica[57].

[1] *Centro Brasileiro de Pesquisas Físicas (CBPF), Rio de Janeiro, Brazil*
[2] *Universidade Federal do Rio de Janeiro (UFRJ), Rio de Janeiro, Brazil*
[3] *Center for High Energy Physics, Tsinghua University, Beijing, China*
[4] *Institute Of High Energy Physics (IHEP), Beijing, China*
[5] *School of Physics State Key Laboratory of Nuclear Physics and Technology, Peking University, Beijing, China*
[6] *University of Chinese Academy of Sciences, Beijing, China*
[7] *Institute of Particle Physics, Central China Normal University, Wuhan, Hubei, China*
[8] *Université Savoie Mont Blanc, CNRS, IN2P3-LAPP, Annecy, France*
[9] *Université Clermont Auvergne, CNRS/IN2P3, LPC, Clermont-Ferrand, France*
[10] *Aix Marseille Univ, CNRS/IN2P3, CPPM, Marseille, France*
[11] *Université Paris-Saclay, CNRS/IN2P3, IJCLab, Orsay, France*
[12] *Laboratoire Leprince-Ringuet, CNRS/IN2P3, Ecole Polytechnique, Institut Polytechnique de Paris, Palaiseau, France*
[13] *LPNHE, Sorbonne Université, Paris Diderot Sorbonne Paris Cité, CNRS/IN2P3, Paris, France*
[14] *I. Physikalisches Institut, RWTH Aachen University, Aachen, Germany*
[15] *Fakultät Physik, Technische Universität Dortmund, Dortmund, Germany*
[16] *Max-Planck-Institut für Kernphysik (MPIK), Heidelberg, Germany*
[17] *Physikalisches Institut, Ruprecht-Karls-Universität Heidelberg, Heidelberg, Germany*
[18] *School of Physics, University College Dublin, Dublin, Ireland*
[19] *INFN Sezione di Bari, Bari, Italy*
[20] *INFN Sezione di Bologna, Bologna, Italy*
[21] *INFN Sezione di Ferrara, Ferrara, Italy*
[22] *INFN Sezione di Firenze, Firenze, Italy*
[23] *INFN Laboratori Nazionali di Frascati, Frascati, Italy*
[24] *INFN Sezione di Genova, Genova, Italy*
[25] *INFN Sezione di Milano, Milano, Italy*
[26] *INFN Sezione di Milano-Bicocca, Milano, Italy*
[27] *INFN Sezione di Cagliari, Monserrato, Italy*
[28] *Università degli Studi di Padova, Università e INFN, Padova, Padova, Italy*
[29] *INFN Sezione di Pisa, Pisa, Italy*
[30] *INFN Sezione di Roma La Sapienza, Roma, Italy*
[31] *INFN Sezione di Roma Tor Vergata, Roma, Italy*
[32] *Nikhef National Institute for Subatomic Physics, Amsterdam, Netherlands*
[33] *Nikhef National Institute for Subatomic Physics and VU University Amsterdam, Amsterdam, Netherlands*
[34] *AGH - University of Science and Technology, Faculty of Physics and Applied Computer Science, Kraków, Poland*
[35] *Henryk Niewodniczanski Institute of Nuclear Physics Polish Academy of Sciences, Kraków, Poland*
[36] *National Center for Nuclear Research (NCBJ), Warsaw, Poland*
[37] *Horia Hulubei National Institute of Physics and Nuclear Engineering, Bucharest-Magurele, Romania*
[38] *Affiliated with an institute covered by a cooperation agreement with CERN*
[39] *DS4DS, La Salle, Universitat Ramon Llull, Barcelona, Spain*

[40] *ICCUB, Universitat de Barcelona, Barcelona, Spain*
[41] *Instituto Galego de Física de Altas Enerxías (IGFAE), Universidade de Santiago de Compostela, Santiago de Compostela, Spain*
[42] *Instituto de Fisica Corpuscular, Centro Mixto Universidad de Valencia - CSIC, Valencia, Spain*
[43] *European Organization for Nuclear Research (CERN), Geneva, Switzerland*
[44] *Institute of Physics, Ecole Polytechnique Fédérale de Lausanne (EPFL), Lausanne, Switzerland*
[45] *Physik-Institut, Universität Zürich, Zürich, Switzerland*
[46] *NSC Kharkiv Institute of Physics and Technology (NSC KIPT), Kharkiv, Ukraine*
[47] *Institute for Nuclear Research of the National Academy of Sciences (KINR), Kyiv, Ukraine*
[48] *University of Birmingham, Birmingham, United Kingdom*
[49] *H.H. Wills Physics Laboratory, University of Bristol, Bristol, United Kingdom*
[50] *Cavendish Laboratory, University of Cambridge, Cambridge, United Kingdom*
[51] *Department of Physics, University of Warwick, Coventry, United Kingdom*
[52] *STFC Rutherford Appleton Laboratory, Didcot, United Kingdom*
[53] *School of Physics and Astronomy, University of Edinburgh, Edinburgh, United Kingdom*
[54] *School of Physics and Astronomy, University of Glasgow, Glasgow, United Kingdom*
[55] *Oliver Lodge Laboratory, University of Liverpool, Liverpool, United Kingdom*
[56] *Imperial College London, London, United Kingdom*
[57] *Department of Physics and Astronomy, University of Manchester, Manchester, United Kingdom*
[58] *Department of Physics, University of Oxford, Oxford, United Kingdom*
[59] *Massachusetts Institute of Technology, Cambridge, MA, United States*
[60] *University of Cincinnati, Cincinnati, OH, United States*
[61] *University of Maryland, College Park, MD, United States*
[62] *Los Alamos National Laboratory (LANL), Los Alamos, NM, United States*
[63] *Syracuse University, Syracuse, NY, United States*
[64] *School of Physics and Astronomy, Monash University, Melbourne, Australia, associated to* [51]
[65] *Pontifícia Universidade Católica do Rio de Janeiro (PUC-Rio), Rio de Janeiro, Brazil, associated to* [2]
[66] *Physics and Micro Electronic College, Hunan University, Changsha City, China, associated to* [7]
[67] *Guangdong Provincial Key Laboratory of Nuclear Science, Guangdong-Hong Kong Joint Laboratory of Quantum Matter, Institute of Quantum Matter, South China Normal University, Guangzhou, China, associated to* [3]
[68] *Lanzhou University, Lanzhou, China, associated to* [4]
[69] *School of Physics and Technology, Wuhan University, Wuhan, China, associated to* [3]
[70] *Departamento de Fisica , Universidad Nacional de Colombia, Bogota, Colombia, associated to* [13]
[71] *Universität Bonn - Helmholtz-Institut für Strahlen und Kernphysik, Bonn, Germany, associated to* [17]
[72] *Eotvos Lorand University, Budapest, Hungary, associated to* [43]
[73] *INFN Sezione di Perugia, Perugia, Italy, associated to* [21]
[74] *Van Swinderen Institute, University of Groningen, Groningen, Netherlands, associated to* [32]
[75] *Universiteit Maastricht, Maastricht, Netherlands, associated to* [32]
[76] *Faculty of Material Engineering and Physics, Cracow, Poland, associated to* [35]
[77] *Department of Physics and Astronomy, Uppsala University, Uppsala, Sweden, associated to* [54]
[78] *University of Michigan, Ann Arbor, MI, United States, associated to* [63]

[a] *Universidade de Brasília, Brasília, Brazil*
[b] *Central South U., Changsha, China*
[c] *Hangzhou Institute for Advanced Study, UCAS, Hangzhou, China*
[d] *Excellence Cluster ORIGINS, Munich, Germany*
[e] *Universidad Nacional Autònoma de Honduras, Tegucigalpa, Honduras*
[f] *Università di Bari, Bari, Italy*
[g] *Università di Bologna, Bologna, Italy*
[h] *Università di Cagliari, Cagliari, Italy*
[i] *Università di Ferrara, Ferrara, Italy*
[j] *Università di Firenze, Firenze, Italy*
[k] *Università di Genova, Genova, Italy*
[l] *Università degli Studi di Milano, Milano, Italy*
[m] *Università di Milano Bicocca, Milano, Italy*
[n] *Università di Modena e Reggio Emilia, Modena, Italy*

[o] *Università di Padova, Padova, Italy*
[p] *Università di Perugia, Perugia, Italy*
[q] *Scuola Normale Superiore, Pisa, Italy*
[r] *Università di Pisa, Pisa, Italy*
[s] *Università della Basilicata, Potenza, Italy*
[t] *Università di Roma Tor Vergata, Roma, Italy*
[u] *Università di Urbino, Urbino, Italy*
[v] *MSU - Iligan Institute of Technology (MSU-IIT), Iligan, Philippines*
[w] *Universidad de Alcalá, Alcalá de Henares , Spain*

[†] *Deceased*

Justification for PRL

This letter presents the LHCb Run 2 legacy measurement of *CP* violation in the benchmark decay $B_s^0 \to \phi\phi$. The measurement precision is significantly improved compared to previous results, and the polarization-dependence of the *CP*-violation parameters in this decay is tested for the first time. This is the most precise determination of time-dependent *CP* violation in any $b \to s$ decay from a single experiment, providing a stringent test of the CKM mechanism and putting severe constraints on new physics model building.

Word count

This letter contains 3885 words in total.
Summary of word counts:
Figures: (300/(1/0.45)+40)+(150/(1/0.6)+20)= 285 word
Tables: 13+14+13+6.5*10= 105 words
Main text: 3495